



POLITECNICO
MILANO 1863

SCUOLA DI INGEGNERIA INDUSTRIALE
E DELL'INFORMAZIONE

EXECUTIVE SUMMARY OF THE THESIS

Magnetolectric nanoparticles as innovative technology for motor nerve stimulation: feasibility assessment through computational methods

LAUREA MAGISTRALE IN BIOMEDICAL ENGINEERING - INGEGNERIA BIOMEDICA

Author: VALENTINA GALETTA

Advisor: PROF. PAOLO RAVAZZANI

Co-advisors: EMMA CHIARAMELLO, SERENA FIOCCHI

Academic year: 2021-2022

1. Introduction

Electrical stimulation is the application of safe levels of electric current for medical purposes. It is a form of physical therapy used to treat both the Central and Peripheral Nervous Systems (CNS and PNS). Particularly, motor nerve stimulation elicits muscle contraction using electric pulses over the peripheral sensory-motor system, contributing to recovery functions, relieving pain, and strengthening the atrophied muscles. Neuroprostheses are devices that integrate electrical stimulation into peripheral neural interfaces. The existing electrodes to use at the interface could be surface, percutaneous, or implantable [1]. Recently, the progress in nano-engineering of magnetolectric (ME) materials opened the path to new stimulating technologies, leading to less invasive but with higher selectivity stimulating approaches, and possibly overcoming the drawbacks of the current approaches. Among all, the innovative core-shell nanoparticles (MENPs) are particularly promising. MENPs consist of a ferromagnetic core and a piezoelectric shell. The magnetolectric effect, i.e. the strain-induced lattice match be-

tween the two magnetostrictive and piezoelectric components, allows the conversion of magnetic to electric energy or vice versa. The magnitude of the linear ME effect in the material is characterized by the magnetolectric coefficient α , defined as the ratio of the polarization change following a change of the magnetic field $\alpha = \Delta\mathbf{P}/\Delta\mathbf{H}$ [V/cmOe] [2]. This innovative technology based on electromagnetic (EM) fields will allow further improve the efficacy of wireless stimulation, thus developing new strategies for stimulating the PNS and CNS, and opening up unprecedented possibilities for biomedical applications. In this framework, computational approaches are a unique tool to evaluate the electric quantities within human tissues and allow for a deep investigation of physical phenomena behind the stimulation effect, thus representing an essential method for the advancement of MENPs toward clinical application.

This work aims to investigate the feasibility of using MENPs as tools for the next generation of bionic interfaces for human arms, by deepening their potential for the electric stimulation of peripheral nerves through a computational approach. This study reports the simulation set-

tings for the computational approach, presenting and discussing the results.

2. Material and Methods

The methodology used to assess the feasibility of using MENPs for the stimulation of peripheral nerves by computational methods consists of two phases of increasing complexity. At first, the simulations presented a very simple framework, with a single MENP and a single motor neuron. Here, both the influence of the MENP-neuron distance and the impact of using different stimulus pulses were explored. Then, a more realistic model of a peripheral nerve was used to investigate the use of either single or multiple MENPs for achieving neural stimulation.

Both analyses consisted of two different steps. The first one involves the resolution of the electric field distribution \mathbf{E} elicited by the MENP in the biological structure, while the second one consists of the neural response determination by the dynamics model of nerve electric behavior. All the simulations have been implemented using the Sim4life platform (by ZMT Zurich Med Tech AG, Zurich, Switzerland, www.zurichmedtech.com).

2.0.1 EM stimulation settings and MENP model

Based on the observation of the distribution of the electric potential on the MENPs surface when subjected to a low amplitude magnetic field, i.e. when ME effect is elicited, it was considered reasonable to approximate the electric behavior of MENPs as dipoles. The geometric structure of the MENPs was a sphere, consisting of two conductive surfaces separated by an insulating layer, as shown in Fig.1. Dirichlet boundary conditions equal to ± 0.5 V were defined over the two surfaces, charging the MENP for a total of 1 V, and the dielectric properties of the techotane material at the MENP stimulating frequency were assigned to the insulating layer. The diameter was set equal to 80 nm.

The ohmic quasi-static approximation was used to solve Maxwell's equations to estimate the \mathbf{E} field distribution, which is the input of the following neural simulations. Dirichlet boundary conditions in which $V = 0$ defined the poten-

tial on the borders of the computational domain. The frequency of the EM stimulation problem was 100 Hz, in the frequency range for neural stimulation [3].

These settings remained unvaried in both simplified and realistic geometry simulations.

2.0.2 Nerve model and neuronal dynamics simulation settings for simplified geometry models

In the simplified geometry models, the system under investigation consisted of a cylindrical structure, of 1000 μm length and 100 μm width, and a single neuronal fiber, of 1000 μm length and diameter equal to 5.7 μm . The tissue of the cylinder was nerve, with electric properties assigned according to literature data [4] at the MENP stimulating frequency.

NEURON computational solver, supplied in Sim4life as a solver library, offered to implement biologically realistic models about the electrical signaling in the axon fiber. It solves computationally the cable equations, aiming both to test hypotheses about the mechanisms that govern the signaling and simulate the membrane potential mechanisms. Among the different models of transmembrane dynamics, the MOTOR MRG model has been chosen thanks to its great physiological accuracy of nerve behavior in human arms. This model is a computer-based double cable model of mammalian nerve fibers modeling the recovery cycle of the axon. Its equivalent circuit consists of explicit representations of the nodes of Ranvier, paranodal and internodal sections of the axon, and a finite impedance myelin sheath. Linear and nonlinear membrane dynamics model the electrical behavior [5].

The titration mechanism implemented in the software was used to estimate the minimum pulse amplitude able to elicit an action poten-

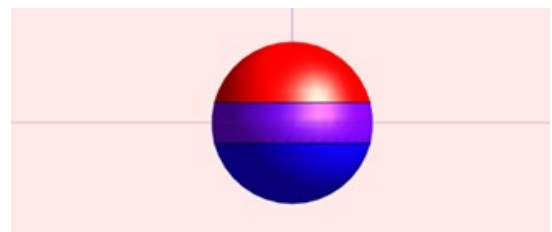


Figure 1: MENP model in Sim4life. Red shell with $V=0.5$ V, Blue shell with $V=-0.5$ V, and insulating layer in purple with techotane material

tial. Titration consists of stimulating the axon with a series of increasing amplitude stimuli, to identify the threshold above which an action potential is generated. It was used in all the simulations of this study, determining the pulse amplitude of the stimulus.

In this simple framework, the influences of the distance and the stimulus pulse shape were separately investigated, and the stimulation settings changed from case to case, as described in the following.

- MENP-fiber distance exploration: one-period sinusoid of 100 Hz as stimulus pulse. Variable distance: 0.5 μm , 1.3 μm , 2 μm , 3.5 μm , 5 μm , 10 μm , 20 μm , and 30 μm .
- Strength-Duration curves and neuron response comparison: one-period sinusoid or single bipolar pulse as stimulus. Frequencies range from 10 to 1000 Hz. MENP-fiber distance equal to 0.5 μm .
- MENP's stimulus polarization: one-period sinusoid of 100 Hz as stimulus pulse. Direct or inverse polarization. MENP-fiber distance equal to 0.5 μm .

In all the simulations, the pulse had duration and time step equal to 200 ms and 0.0025 ms, respectively.

2.0.3 Nerve model and stimulation settings for realistic geometry models

Further in the study, the system under investigation was more detailed, accounting for the realistic anatomy of a peripheral nerve. The system consisted of a cylindrical model in a saline solution, and its tissues were the saline solution, the nerve, the interstitial layer, three different connective tissues, three different blood vessels, and seven fascicles of fibers. Their dielectric properties were assigned according to literature data [4] at the MENP stimulating frequency. The axon properties are constant along its length, the layers of tissue surrounding the fascicles and nerves have circular symmetry, and the fibers are modeled with a MRG model and a diameter of 5.7 μm .

The stimulus pulse was a one-period sinusoid, with an amplitude equal to the one obtained by the EM simulation, a frequency of 100 Hz, and duration and time step equal to 200 ms and 0.0025 ms, respectively.

In the simulations, the number of MENPs was

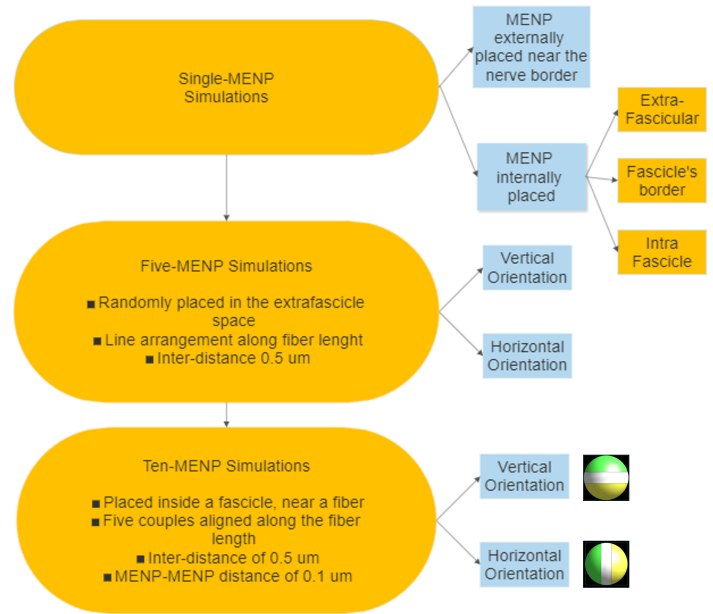


Figure 2: Flowchart illustrating the workflow of the realistic model simulations.

one, five, or ten, and their position and orientation varied. Fig. 2 illustrates the workflow and the stimulation settings.

3. Results

The analysis of results will consider separately the resulting \mathbf{E} field distribution on the nerve, the titration factor as an estimation of the amplitude of the stimulus needed to elicit the action potential, and the neuron response differentiating the simulations.

At first, the outcomes of the simple geometry are reported. When investigating the influence of the MENP-axon distance, the \mathbf{E} field distribution was studied everywhere around the MENP. The focus moved toward a slice view over the YZ plane, which comprises the nerve along its full length, and among all the possible YZ planes, the section that holds the maximum RMS of \mathbf{E} amplitude (V/m) was chosen for the study. The colormap ranged between 0 and 10^4 V/m, as visible in Fig. 3. Particular attention was to the overall field of the RMS of \mathbf{E} along the neuron length. In all eight different simulations, a similar bell shape of the distribution over the neuron length was shown, highlighting a change in the bell's width and its maximum amplitude. By increasing the MENP–neuron distance, the bell shape was wider but the maximum amplitude of the \mathbf{E} field substantially decreased. The peak

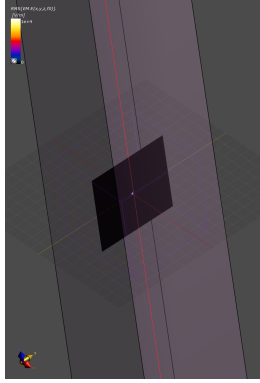


Figure 3: View of the RMS of \mathbf{E} amplitude. Visualization on the YZ plane, particularly the plan with maximum RMS \mathbf{E} amplitude. The red line corresponds to the position of the neuron, and it's the line along with the \mathbf{E} field is analyzed.

values of the distributions were 20929.8 V/m, 466.5 V/m, 157.2 V/m, and 30.7 V/m and the bells' widths quantified at the 10% of the maximum amplitude were 1.8 μm , 7 μm , 9.5 μm and 14.8 μm for the distances 0.5 μm , 1.3 μm , 2 μm and 3.5 μm , respectively. An example is shown in Fig.4. Results highlighted the influence of the MENP-axon distance, the pulse shape, and its polarization over the titration value. As well expected, increasing the distance, the titration factor increases, so a bigger stimulus amplitude is necessary to stimulate the neuron. The value ranges from 3.16 to 362 for an interposed distance between 0.5 and 3 μm . The time of the first spike was not affected. The inverse polarization of the pulse determines instead a slight decrease in the titration value and a strong increase in the time of the first spike. For the same interposed distance, between 0.5 and 3 μm , the needed amplitude value ranges from 3.02 to 346, whereas the time interval before the start of the spiking activity almost doubled. In the end, the comparison of the SD curves when stimulating with a sinusoidal or bipolar pulse, shown

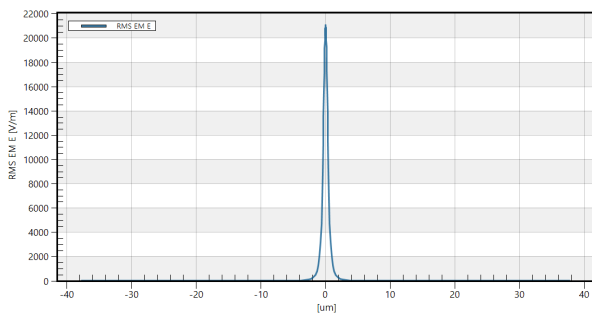
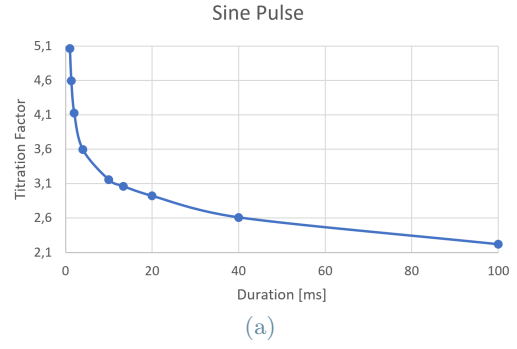
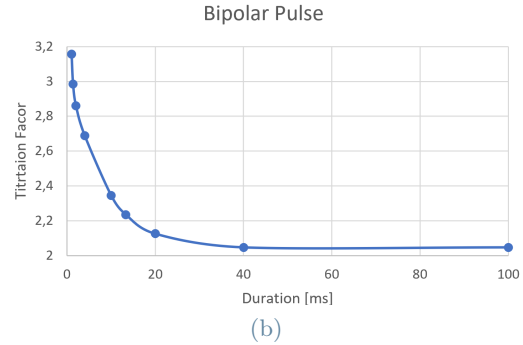


Figure 4: Overall field of the RMS of E analyzed along the neuron for the MENP-neuron distances of 0.5 μm



(a)



(b)

Figure 5: Strength-Duration curves comparison: stimulus duration in ms on the x-axis, and titration factor on the y-axis. The delivered pulse was sinusoidal, on the top, or bipolar, on the bottom. Points at frequencies of 10, 25, 50, 75, 100, 250, 500, 750, and 1000 Hz are highlighted.

in Fig.5, underlined the influence of the pulse shape over the titration factor. Smaller values are needed when stimulated with a bipolar pulse. The response of the neuron in terms of transmembrane potential, has the characteristic shape of an action potential, as shown in Fig.6 for the distance of 0.5 μm . Negligible differences in the shape of the action potential were observed when considering different distances between MENP and the nerve, and when varying the pulse shape or polarization. Dissimilarities in the plots were observed concerning the beginning of the spiking time. An increase in the time

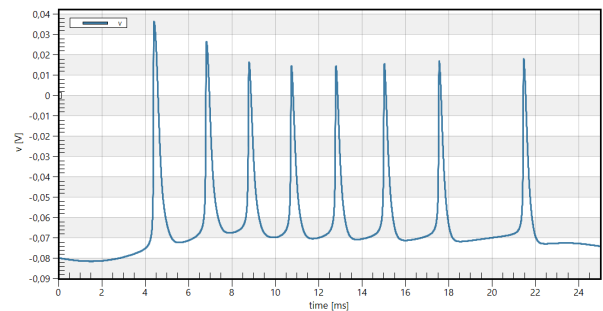


Figure 6: Neural response, in terms of transmembrane potential (V) during the stimulation. The MENP-neuron distance was 0.5 μm .

of the first spike corresponds to a decrease in the pulse frequency or to the inverse pulse polarization.

Then, the results of the realistic simulations will be presented. Depending on the configuration, the slice view where to focus to study the \mathbf{E} field was differently oriented in the space, but the overall distribution was always analyzed on the plane that holds the maximum RMS of \mathbf{E} amplitude (V/m). The analysis highlighted the influence of the interposed tissue on the field distribution, as well as the importance of MENPs vicinity and orientation. More in detail, an inhomogeneous medium causes an asymmetrical \mathbf{E} field distribution, whereas the MENPs interaction and 90° -rotation strongly affect the EM distribution. Examples are shown in Fig.7. The overall field of the RMS of \mathbf{E} along the neuron length was studied for the ten-MENP configuration. The distribution is now imitating a pulse shape, and the amplitude changes depending on MENPs' orientation. Peak values were lower with MENPs vertically oriented.

The titration factor, analyzed for all the fibers in all the fascicles, varied, depending on the MENPs' arrangement (both number, position, and orientation). Considering the single MENP simulations, the biggest values refer to the MENP positioned on the border of the MENP, and the lowest to intrafascicular simulation. Higher intensity is needed when the MENP is placed on the border of the fascicle than when the MENP is placed extrafascicular. As an example, titration values necessary to activate one of the fibers were $3.67 \cdot 10^6$, 382976, 475136, and 313344 for the MENP placed near the border of the nerve, extrafascicularly, on the border of a

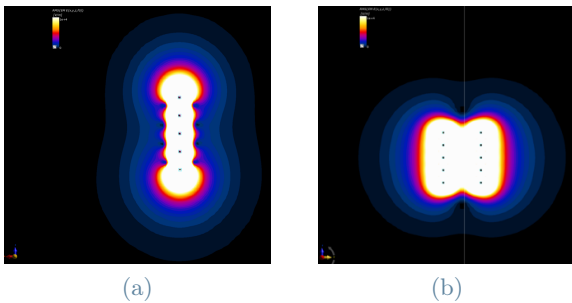


Figure 7: View of the RMS of \mathbf{E} distribution. a) View of the XZ plane in the configuration with five MENPs oriented vertically. b) View of the YZ plane in the configuration with ten MENPs horizontally oriented.

fascicle, and intrafascicular, respectively. As expected, the titration value decreases by increasing the number of MENPs. Considering another neuronal fiber, the titration factor decreased from 47872 to 2512 when stimulated with a single MENP or ten MENPs placed intrafascicular. In the end, a 90° -rotation decreases the needed amplitude value. For the same fiber mentioned before, the needed stimulus amplitude increased from 2512 to 286720 from the vertical to the horizontal orientation. The node of the first spike varied by changing the MENPs' position and orientation.

The analysis will be concluded by showing the neuron response, an example is illustrated in Fig.8. For all the fibers in every simulation, the neuron behavior shows the characteristic shape of an action potential. Negligible distinctions were in the spiking, which instead reflects the different times of the first spike. No influences of the MENPs configurations over the fiber response have been highlighted.

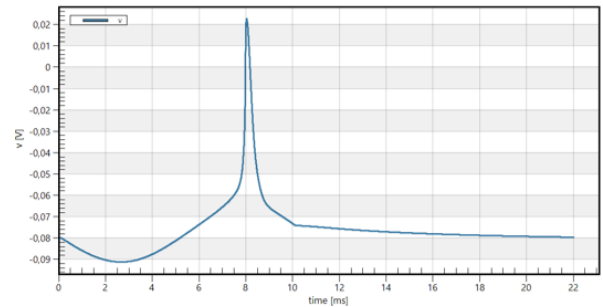


Figure 8: Typical neuron response.

4. Discussion and Conclusion

In summary, the computational approaches have proven the feasibility of using MENPs as tools for the electric stimulation of peripheral nerves. At first, simplified simulations demonstrated the influence of MENP-axon distance, the pulse shape, and the pulse polarization over the EM field distribution and the axon response. Results showed how the MENP-axon distance impacts the amplitude of the peak of the EM field distribution but not the shape of the distribution itself. The overall field analyzed along the neuron demonstrated how punctual stimulation is feasible with MENP, allowing a very high spatial resolution. Particularly, it was highlighted how the spatial resolution and the field intensity decrease by increasing the distance. The

MENP capability to induce an action potential in the nerve was confirmed, and the response of the nerve was characterized. It was confirmed how the MENP-axon distance, the pulse shape, and its polarization don't have any influence on the action potential shape, but the dependence of the variation of the time of the first spike on the stimulus frequency was evidenced. Finally, the titration factor gives information about the amplitude needed for the stimulus of the MENP. As expected, results confirmed how the needed pulse amplitude increases by increasing the MENP-axon distance. Moreover, it was discovered that the titration factor is affected by the pulse shape and the pulse polarization. Future work can address the feasibility of different stimulating settings with MENPs. Once the investigation has emphasized the nerve response and the EM distribution in a simplified environment, the study continued in a more realistic model, to deepen the impact of using MENPs as stimulating tools. Simulations with one, five, or ten MENPs were run, and the results of the EM field distribution, nerve response, and titration factor were compared. It was demonstrated how the \mathbf{E} field is affected by the number, position, and orientation of MENPs, as well as the homogeneity or inhomogeneity of the medium. The needed titration factor was compared between different simulations. As expected, its value decreases by increasing the number of MENPs. Some unattended results underlined the importance of the position where to place the MENPs for stimulation. In fact, the high spatial resolution is not sufficient if the MENPs arrangement is not optimized along the nerve. In the future, studies can focus on the development of MENPs chains or nanostructures with MENPs in order to get a highly effective stimulation to the positions of the nodes, without losing spatial resolution. In the end, the neuron response was characterized, and the usual action potential shape was evidenced.

In conclusion, this study demonstrated the feasibility of using MENPs as tools for the stimulation of peripheral nerves, highlighting all their potentialities. A lot is still to be understood about their functioning, and future work will be needed. The application of this innovative technology in medicine and bio-robotics will address the current limitations and drawbacks of

the actual stimulating approaches, giving rise to cutting-edge bio-hybrid interfaces between living and artificial systems.

5. Acknowledgements

The authors wish to thank ZMT Zurich MedTech AG (www.zmt.swiss) for providing SIM4Life software.

This research was in the framework of one of the ongoing projects "Fit4MedRob- Fit for Medical Robotics" Grant (contract number CUP B53C22006960001) financed by the Italian Ministry of Research (MUR) under the complementary actions to the NRRP (PNC0000007).

References

- [1] Aikaterini D. Koutsou, Susanna Summa, Bilal Nasser, Josefina Gutierrez Martinez, and Muthukumaran Thangaramanujam. Upper Limb Neuroprostheses: Recent Advances and Future Directions. In José L Pons and Diego Torricelli, editors, *Emerging Therapies in Neurorehabilitation*, volume 4, pages 207–233. Springer Berlin Heidelberg, Berlin, Heidelberg, 2014. Series Title: Biosystems & Biorobotics.
- [2] Sakhrat Khizroev. Technobiology's Enabler: The Magnetoelectric Nanoparticle. *Cold Spring Harbor Perspectives in Medicine*, 9(8):a034207, August 2019.
- [3] Marta Pardo and Sakhrat Khizroev. Where do we stand now regarding treatment of psychiatric and neurodegenerative disorders? Considerations in using magnetoelectric nanoparticles as an innovative approach. *WIREs Nanomedicine and Nanobiotechnology*, 14(3), May 2022.
- [4] Baumgartner C Neufeld E Lloyd B Goselin MC Payne D Klingenberg A Kuster N Hasgall PA, Di Gennaro F. It's database for thermal and electromagnetic parameters of biological tissues. Version 4.1, February 2022.
- [5] Cameron C. McIntyre, Andrew G. Richardson, and Warren M. Grill. Modeling the Excitability of Mammalian Nerve Fibers: Influence of Afterpotentials on the Recovery Cycle. *Journal of Neurophysiology*, 87(2):995–1006, February 2002.